1-1-2008

Potential energy curves and electronic structure of 3d transition metal hydrides and their cations

Satyender Goel
University of Central Florida

Artëm E. Masunov
University of Central Florida

The Journal of Chemical Physics

Potential energy curves and electronic structure of $3d$ transition metal hydrides and their cations

Cite as: J. Chem. Phys. **129**, 214302 (2008); https://doi.org/10.1063/1.2996347
Submitted: 09 July 2008 . Accepted: 16 September 2008 . Published Online: 02 December 2008

Satyender Goel, and Artëm E. Masunov

Potential energy curves and electronic structure of 3*d* transition metal hydrides and their cations

Satyender Goel[1] and Artëm E. Masunov[2,a)]
[1]*Nanoscience Technology Center and Department of Chemistry, University of Central Florida, Orlando, Florida 32826, USA*
[2]*Nanoscience Technology Center, Department of Chemistry, and Department of Physics, University of Central Florida, Orlando, Florida 32826, USA*

(Received 9 July 2008; accepted 16 September 2008; published online 2 December 2008)

We investigate gas-phase neutral and cationic hydrides formed by 3*d* transition metals from Sc to Cu with density functional theory (DFT) methods. The performance of two exchange-correlation functionals, Boese–Martin for kinetics (BMK) and Tao–Perdew–Staroverov-Scuseria (TPSS), in predicting bond lengths and energetics, electronic structures, dipole moments, and ionization potentials is evaluated in comparison with available experimental data. To ensure a unique self-consistent field (SCF) solution, we use stability analysis, Fermi smearing, and continuity analysis of the potential energy curves. Broken-symmetry approach was adapted in order to get the qualitatively correct description of the bond dissociation. We found that on average BMK predicted values of dissociation energies and ionization potentials are closer to experiment than those obtained with high level wave function theory methods. This agreement deteriorates quickly when the fraction of the Hartree–Fock exchange in DFT functional is decreased. Natural bond orbital (NBO) population analysis was used to describe the details of chemical bonding in the systems studied. The multireference character in the wave function description of the hydrides is reproduced in broken-symmetry DFT description, as evidenced by NBO analysis. We also propose a new scheme to correct for spin contamination arising in broken-symmetry DFT approach. Unlike conventional schemes, our spin correction is introduced for each spin-polarized electron pair individually and therefore is expected to yield more accurate energy values. We derive an expression to extract the energy of the pure singlet state from the energy of the broken-symmetry DFT description of the low spin state and the energies of the high spin states (pentuplet and two spin-contaminated triplets in the case of two spin-polarized electron pairs). The high spin states are build with canonical natural orbitals and do not require SCF convergence. © *2008 American Institute of Physics*. [DOI: 10.1063/1.2996347]

I. INTRODUCTION

The studies of transition metal (TM) systems present a challenge for theoretical description due to the presence of several closely spaced electron states, which results in strong electron correlation.[1–3] For this reason molecules containing TMs serve as an important testing ground for various methods in theoretical chemistry and molecular physics. Transition metal hydride (TMH) is a small enough system to apply sophisticated and computationally demanding methods of the wave function theory (WFT). This is one of the reasons why TMHs and their positive ions have been investigated repeatedly. Availability of these results presents an excellent opportunity to validate new theoretical methods, including various density functional theory (DFT) approaches.

Besides theoretical interest, chemical bonds between TM atom and hydrogen play an important role in applications, including surface chemistry and nanoparticle cluster catalysis, which fostered research on TMHs and their cations.[4] The importance of TMHs, such as iron hydride (FeH) in Astrophysics presents an additional motivation to study its spectroscopic constants and potential energy curves (PECs).[5–7] Ni is another important TM due to its catalytic properties. The electronic structure of NiH was investigated using self-consistent field (SCF)/configuration interaction (CI) methods three decades ago[8] and more recently with other multireference methods with or without relativistic effects.[9–11] PECs had been also calculated for other first row TMHs, including TiH,[12–14] CoH,[15] CuH,[11,16] VH,[17] and ScH.[18] Walch and Bauschlicher[17] used complete active space self consistent field singly and doubly substituted configuration interaction (CASSCF/SDCI) method to account for both static and dynamic electron correlation effects in the ground state of most of the first row TMHs (TiH, VH, CrH, MnH, FeH, NiH). The related method multi-configuration self-consistent field second order configuration interaction (MCSCF/SOCI) was used by Koseki *et al.*[19] to study both ground and excited state PECs of the five first row TMHs (ScH, TiH, VH, CrH, MnH) recently.[20,21]

Besides the neutral TMHs, gas-phase cations of TMHs attracted considerable interest as simplest compounds containing TM in different oxidation states in the hope that this study can help in understanding the behavior of more com-

a)Author to whom correspondence should be addressed. Electronic mail: amasunov@mail.ucf.edu.

plicated systems. TM compounds of interest include systems used in surface and homogeneous catalyses[4] and metalloenzymes.[22] The comparison of bond energies and bond lengths of first row (Sc–Zn) TMHs calculated with modified coupled pair functional (MCPF) (Ref. 23) method and generalized valence bond[24] formalisms had shown good agreement with experiment. A few extensive potential energy surface studies have been carried out for TMH positive ions such as FeH^+,[25] CoH^+,[26] CrH^+,[27] and TiH^+.[28]

Density functional theory (DFT)[29,30] combined with approximate exchange-correlation (XC) functionals[31] has become a method of choice for the calculation of numerous properties of molecules and solids. Unlike modern semiempirical methods such as modified scaled intermediate neglect of differential overlap (MSINDO) (Ref. 32) and density functional tight binding (DFTB),[33] it does not require tedious empirical parameter fitting to produce acceptable results. Another advantage of DFT is the relatively low computational cost as compared to high level multireference *ab initio* methods of WFT.[34] Although multireference techniques can accurately describe the molecular wave function at all interatomic distances, they are computationally very expensive. With increase in system size WFT become unfeasible and DFT remains the only first principles method available. This motivated extensive efforts in development and testing of various functionals and formalisms within DFT. Unlike WFT methods, DFT accounts for electron correlation not through increasing complexity of the wave function but via approximate XC functional. The need to improve XC functionals arises from known deficiencies of DFT describing so-called strongly correlated systems where vacant and occupied electronic levels approach degeneracy (this effect is also known as static or nondynamic electron correlation). This situation is observed in *d*- and *f*-electron systems or when chemical bonds are being stretched. Despite these limitations, different XC functionals are widely used for modeling of various systems. Early XC functionals were dependent only on electron density [local spin density approximation (LSDA)]. The next generation of XC functionals also included energy dependence on the gradient of the density [generalized gradient approximation (GGA)]. Among the later developments are kinetic energy density dependent functionals, which are also known as meta-GGA, including Tao–Perdew–Staroverov-Scuseria (TPSS) and BB95.[35,36] GGA and meta-GGA functionals are called semilocal functionals to distinguish them from local density approximation (LDA), on one hand, and nonlocal functionals including orbital dependence, on the other hand.

All LSDA, GGA, and meta-GGA are known to underestimate band gaps in solids. On the other hand, the Hartree–Fock (HF) method yields an overestimated band gap. Adding a fraction of HF exchange to DFT (known as hybrid DFT) improves the agreement of predicted band gap values with experimental ones.[37,38] Hybrid DFT can be theoretically justified based on adiabatic connection arguments.[35] Examples of successful hybrid functionals development include B3LYP (Ref. 39) and PBE0.[40]

In the past decade TMHs had been used to investigate the accuracy and efficiency of DFT methods. Ziegler and Li[41] studied TMH cations by using LDAs and GGA. They found bond lengths to be in agreement with experimentally determined values, but their dissociation energies were less accurate. Barone *et al.*[42] used pure and hybrid DFT functionals BLYP and B3LYP to study TM complexes, which include first row TMHs and their cations. B3LYP was found to give accurate dissociation energies but somewhat overestimate the bond lengths and dipole moments. In a detailed study of 3*d* TM systems including monohydrides, Furche and Perdew[1] were not able to reproduce these dissociation energies with the same functionals and basis sets. Presumably, their SCF procedure systematically converged to a different local minimum as spin-adapted (SA) unrestricted Kohn–Sham (UKS) was used by Barone *et al.*[42] and broken-symmetry (BS) orbitals were used by Furche and Perdew.[1] Among various semilocal (BP86, PBE, TPSS) and hybrid density functionals (B3LYP, TPSSh), Furche and Perdew[1] recommended semilocal DFT functional TPSS as the workhorse of TM compounds. Their recommendation was based on the price/performance ratio, even though the hybrid functionals achieve a lower mean absolute error in bond energies. Jensen *et al.*[3] investigated the performance of five different density functionals (B3LYP, BP86, PBE0, PBE, BLYP) for diatomics of first row TM systems. They concluded that the success of a functional is system specific, which means that all of these functional are more accurate for certain systems and less accurate for others. Jensen *et al.*[3] suggested an alternative way to get to the correct energies by taking the arithmetic average of the functionals, which under- and overestimate the energies. Baker and Pulay[43] studied metal hydrides (MHs) and methylates MCH_3 (both neutral and cations) with two new functionals OLYP and O3LYP but found no advantage compared to BLYP and B3LYP. Riley and Merz[44] recently published a DFT study with 12 different functionals on several small TM molecules including five TMHs. They concluded that inclusion of exact exchange generally gives more consistently accurate results for heats of formation and ionization energies in TM systems. They also found B3LYP/6-31G** to be the best for ionization potentials (IPs) and PBE0/6-31G** to be the best for heats of formations.

DFT studies mentioned above used different basis sets and XC functionals and more importantly different protocols to obtain SCF solutions. The protocol includes the SA or BS approach, wave function stability check, and initial guess. All these details may result in the large differences in calculated values for TM systems. Yet, they are rarely mentioned explicitly. Only a few papers mentioned how the lowest-energy SCF solution is obtained. For instance, Schultz *et al.*[45] reported using orbitals from CrMn as initial guess for Cr_2 to obtain the BS solution. Another example is constrained DFT calculations of Ni_2 and NiH by Diaconu *et al.*,[46] where orbitals obtained from Ni atom were used as initial guess. The symmetry of electronic states was reported by Barone and Adamo,[47] which indicates that lower-energy BS solutions were not attempted. On the other hand, Furche and Perdew[1] systematically considered all possible microstates, corresponding to distribution of the metal va-

lence electrons over 4*s* and 3*d* shells, converged them individually in SCF procedure, and selected the one with the lowest energy.

Also, the studies described above employed spin-polarized (or unrestricted) KS formalism and ignored spin contamination. Spin contamination plays a major role in describing energy deviation of the systems with the possibility of exhibiting more than one multiplicity, largely in complex systems involving TM compounds. The present study takes into consideration the spin correction detailed in the Appendix.

In this study we use both pure meta-GGA and hybrid meta-GGA XC functionals TPSS and Boese–Martin for kinetics (BMK) to compare their performance with WFT methods and experimental data. To provide insight into some of the important concepts, we focus here on TMH and TMH^+ (first row of TMs), examine the lowest states in several spin multiplicities and analyze variations in bond energies, bond lengths, and electron densities. PECs and effect of spin correction are discussed. The DFT results are compared to experiment and WFT calculations.

TPSS (Ref. 48) (meta-GGA functional) was designed to correct the too-large atomization energies and increase the too-small jellium surface energies obtained with local spin density (LSD) (jellium is the model system of interacting electrons and a uniform background of positive charge). It had been shown to accurately predict bond energies and bond lengths in molecules, hydrogen-bonded complexes, and ionic solids.[1] The performance of TPSS approaches that of the hybrid PBE0 functional with a practical advantage of not including HF exchange.[48]

BMK is a hybrid meta-GGA functional designed to be superior in describing transition state properties as well as atomization energies, geometry, and harmonic frequencies of the molecules in the ground state.[49] The BMK functional was developed based on a diverse and balanced parametrization set including TM complexes and hydrogen-bonded systems. However, the performance of BMK for TM systems varies.[50]

II. COMPUTATIONAL DETAILS

All calculations were done with the GAUSSIAN03 (Ref. 51) program using all-electron Wachters+*f* (Refs. 52 and 53) basis set. Spin-polarized (unrestricted) DFT was used throughout. The initial guess was generated by using the Harris functional,[54] which is the default option in GAUSSIAN03. SCF convergence threshold was set to 10^{-7} and relaxed to 10^{-5} in a few problematic cases. The initial guess was followed by either geometry optimization or scan along the interatomic distance to plot the PEC. In some cases (CrH, VH), the Harris guess lead to SCF convergence problems, and HF orbitals were used as a guess. In a few cases where geometry optimization was terminated due to convergence failure, converged KS orbitals were used as the initial guess (BMK orbitals in the case of TPSS nonconvergence and vice versa).

A potential complication in the study of systems with nearly degenerate energy levels is the danger of obtaining distinctly different SCF solutions. When different solutions are obtained for the equilibrium geometry and for the dissociation limit, the energy difference is no longer physically meaningful. In order to ensure consistency of SCF solution for all geometries, we built entire PECs and verified that it does not have discontinuities, indicating the switch from one SCF solution to another. To avoid false SCF solutions with Fermi holes (i.e., virtual orbitals with energy lower than some of the occupied ones), a new SCF algorithm making use of fractional occupation numbers (FONs) around the Fermi energy was employed. This was accomplished by using the keywords SCF=Fermi and IOp(5/22=5). In the FON approach the orbital occupations are determined using the Fermi–Dirac function for a fictitious electron temperature, so that the sum of occupation numbers equals the correct number of electrons for the system.[55] The electron temperature value was set to 3000 K at the initial SCF cycle and lowered to 0 K in ten SCF steps, so that the occupational numbers became integer at the final SCF cycles. The stability of the SCF solution was checked, and KS orbitals were reoptimized (if unstable) using the keyword Stable=Opt. Default integration grid was used for all the calculations.

The Molden[56] graphical interface was used to examine KS orbitals at the dissociation limit, as well as at the points where potential energy curves were found to be nonmonotonic. For one case (CrH), in order to obtain SCF solution with the lower energy, spin polarization of σ bond had to be inverted to have minority spin density localized on H atom using the keyword Guess=Alter. Natural bond orbital (NBO) analysis due to Reed and Weinhold[57] was used to interpret the electron density. The NBOs are obtained by unitary transformation of occupied molecular orbitals (MOs) so that they block diagonalize the (alpha and beta) density matrices and give the best Lewis representation of the electronic structure. Relativistic calculations were done with the second-order Douglas–Kroll approximations[58,59] using the keyword Int=DKH.

III. RESULTS AND DISCUSSIONS

A. Neutral metal hydrides

1. Binding energies

Dissociation energies for neutral hydrides in equilibrium geometry are reported in Table I and Fig. A1.[60] Comparisons with three sets of experimental data and some of the published WFT and DFT predictions are also listed. To calculate the root mean square (rms) deviations for all theoretical values we used two sets of experimental data, compiled by Barone and Adamo[47] and Furche and Perdew,[1] and the third set presents our compilation of the original experimental data including the error bars.

Based on rms values (last three columns in Table I), BMK gives the best agreement with experiment, followed by two WFT methods. The other DFT methods range as follows. Among BS methods, the accuracy quickly deteriorates as the fraction of HF exchange decreases from BMK (42%) to B3LYP (20%) to TPSSh (10%) to TPSS (0%). SA formalism, on the other hand, shows only marginal improvement

TABLE I. Dissociation energies (kcal/mol) of neutral TMHs and rms deviations from the experimental values.

	ScH		TiH	VH		CrH			MnH		FeH	CoH	NiH	CuH	rms deviations		
Multiplicity	1	3	4	3	5	2	4	6	5	7	4	3	2	1	Set 1	Set 2	Set 3
BS-TPSS	95.5	64.9	67.8	59.4	64.6	68.3	55.9	57.9	53.0	52.8	60.9	65.7	76.1	69.0	6.62	7.37	7.75
BS-BMK	50.8	50.2	48.7	43.6	55.7	43.7	48.1	52.5	37.2[a]	34.8	41.0	46.4	59.5	61.8	1.79	1.06	1.38
SA-BLYP[b]	42.4		55.7		66.7			57.0		26.5	42.3	47.4	68.1	66.2	3.93	2.44	2.90
SA-B3LYP[b]	40.2		60.1		63.8			54.0		34.8	40.5	43.4	60.3	63.5	3.09	2.23	2.56
BS-B3LYP[c]	57.8		66.8		62.9			54.9		39.4	55.3	61.6	60.9	62.7	4.97	3.67	4.12
BS-TPSSh[c]	62.8		68.2		64.2			55.9		50.9	59.6	62.9	64.2	65.5	5.80	4.77	5.22
MCSCF+SOCI [d]	47.3		43.3	36.6	42.7		37.8	44.2	21.8	33.6					1.73	2.32	1.84
MCPH[e]	51.0		47.3		53.0			48.7	21.9	39.4	45.0	44.7	64.3	61.6	1.84	1.38	1.63
BS-TPSS:DKH	95.2	64.1	71.8	58.3	66.0	65.9	56.9	59.0	50.5	51.7	61.8	67.1	71.9	71.7	6.93	7.52	7.91
BS-BMK:DKH	51.9	49.0	49.1	45.6	51.9	50.4	46.0	54.2	33.9	33.7	40.8	42.9	60.7	63.9	1.85	1.19	1.42
Expt. set 1[b]			45.2		49.1			44.5		39.0	34.4	42.9	56.5	60.0			
Expt. set 2[c]	47.5		50		51.4			46.8		31.1	39.2	48.4	61.3	63.4			
	47.5		48.9		49.1			44.5[f]		30.2	37.5	46.0	59.4	61.0			
Expt. set 3	±2.0[g]		±2.1[h]		±1.6[f]			±1.6 [f]		±4.4[i]	±1.9[j]	±3.0[k]	±3.0[k]	±4.0[k]			

[a]Spin corrected, using the scheme detailed in the Appendix.
[b]Reference 47.
[c]Reference 1.
[d]References 19–21.
[e]Reference 79.
[f]Reference 64.
[g]Reference 63.
[h]Reference 62.
[i]Reference 65.
[j]Reference 66.
[k]Reference 61.

from pure BLYP to hybrid DFT (B3LYP). SA-B3LYP gives 80% lower rms value than BS-B3LYP, but it is still twice less accurate than BS-BMK.

The individual values of deviations are plotted in Fig. A1.[60] One can see that BMK values are within 4 kcal/mol of experimental ones for almost all the systems (8 kcal/mol for CrH). Scalar relativistic correction does not improve the energies, and deviations are similar to the one observed in nonrelativistic BMK. TPSS strongly overbinds in all cases, and the deviations are from 10 to 20 kcal/mol with ScH showing largest of all (48 kcal/mol), and 10% of HF exchange in TPSSh does not improve the situation. A small fraction of HF exchange (TPSSh) helps only in the case of NiH, while a larger fraction helps in most cases. SA formalisms (BLYP and B3LYP) are close to each other for all systems, except for MnH, but have no systematic deviations otherwise. All DFT methods agree for full and half-full d shells (CuH and CrH), although this consensus is ~10 kcal/mol away from experimental value[61–66] in the case of CrH. WFT and BMK are everywhere close to the baseline with MCPF slightly overbinding and MCSCF+SOCI slightly underbinding. The first two (ScH, TiH) and last three systems (CoH, NiH, CuH) are especially well reproduced.

In the past, relativistic corrections were reported to be important in the systems involving $3d$ TMs.[45,67,68] We studied scalar relativistic effects on the dissociation energies with Douglas–Kroll[58] approximations and found them to be close to 2 kcal/mol. Moreover, we find that relativistic correction does not improve the agreement with experiment. This is in sharp contrast with s/d excitation energies in $3d$ atoms, which were reported to improve nearly twice when scalar relativistic effects are taken into account. For the nickel hydride the scalar relativistic corrections of the WFT theory level were calculated by Marian *et al.*[10] They compared the results of the conventional perturbative method to the variational ones and found the coupling between the relativity and electron correlation to be very similar, despite the fact that relativity accounts for unusually large, 0.36 eV, increases in splitting between the nearly degenerate d^8s^2- and d^9s^1-derived levels. Although Marian *et al.*[10] did not discuss the binding energies, in a later work Pouamerigo *et al.*[11] found the relativistic corrections to increase the dissociation energy by 2.5 kcal/mol for NiH and by 2.3 kcal/mol for CuH at the CASPT2 level, bringing it closer to the experimental values. We attribute the absence of improvement in our calculated D_e to the fact that spin-orbit (SO) effects are not accounted for. To take SO coupling into accounts, Diaconu *et al.*[46] used weighted averages over J components of the experimental data for easy comparison with the nonrelativistic calculations. Unfortunately, the fine splitting in TMHs (necessary to use this technique) are only available for some of the hydrides [NiH,[69,70] CoH,[71] FeH (Ref. 72)] but not for others. Schultz *et al.*[45] corrected their DFT binding energies by adding SO corrections term defined by the equation $\Delta E_{SO}=nE_{SO}(L)+E_{SO}(M)-E_{SO}(ML_n)$, where three different SO energies are defined for a general process given by $ML_n \rightarrow M+nL$. They have used atomic spectral information listed in Moore's[73] books and equations from Herzberg's[74] books to calculate SO effects for FeH and CoH to −0.12 and −0.37 kcal/mol.

2. Bond lengths

Equilibrium bond lengths are reported in Table II and Fig. A2.[60] Scalar relativistic corrections with BMK show smaller rms deviations, almost half of the ones compared to nonrelativistic-BMK and WFT methods. Curiously, all nonrelativistic methods demonstrate the same accuracy.

TABLE II. Equilibrium bond lengths (Å) of neutral TMHs and rms deviations from the experimental values.

	ScH		TiH	VH		CrH			MnH		FeH	CoH	NiH	CuH	
Multiplicity	1	3	4	3	5	2	4	6	5	7	4	3	2	1	rms
BS-TPSS	1.798		1.756	1.678	1.684	1.633	1.629	1.654	1.590	1.713	1.554	1.523	1.472	1.475	0.0080
BS-BMK	1.755	1.874	1.783	1.712	1.705	1.642	1.658	1.668	1.745	1.745	1.581	1.525	1.486	1.506	0.0079
SA-BLYP[a]	1.743		1.750		1.681			1.652		1.720	1.561	1.510	1.507	1.460	0.0080
SA-BSLYP[a]	1.730		1.744		1.677			1.654		1.723	1.561	1.510	1.509	1.460	0.0080
BS-B3LYP[b]			1.760					1.663		1.734	1.571	1.524	1.516	1.482	0.0084
BS-TPSSh[b]								1.659		1.720	1.570	1.526	1.505	1.479	0.0076
MCSCF+SOCI [c]	1.782		1.852		1.758		1.658	1.676	1.644	1.702					0.0202
MCPF[d]	1.800		1.840		1.740			1.700	1.644	1.770	1.580	1.532	1.439	1.458	0.0107
BS-TPSS:DKH	1.795		1.754	1.677	1.681	1.637	1.621	1.646	1.582	1.709	1.555	1.506	1.455	1.456	0.0090
BS-BMK:DKH	1.756	1.875	1.783	1.714	1.728	1.747	1.659	1.660	1.652	1.740	1.574	1.513	1.467	1.484	0.0045
Expt.								1.662[e]		1.740[e]	1.589[f]	1.513[g]	1.475[e]	1.463[h]	

[a]Reference 47.
[b]Reference 1.
[c]References 19–21.
[d]Reference 79.
[e]Reference 75.
[f]Reference 76.
[g]Reference 77.
[h]Reference 78.

Table II includes experimental data available[75–78] for six TMH systems out of nine in the 3*d* TM series. BMK relativistic bond lengths (Fig. A2[60]) for CrH, MnH, CoH, and NiH are in very good agreement with experimental values, while WFT shows the largest deviations for the same four systems. For FeH and CuH, the deviations of 0.015 and 0.021 are obtained with BMK-DKH, where WFT deviations are somewhat smaller (0.009 and 0.005, respectively).

3. Potential energy curves and spin gaps

PECs for neutral hydrides of ScH, VH, MnH, and CrH in various multiplicities are reported in Figs. A3–A5[60] and Fig. 1, together with available MCSCF+SOCI curves. All the curves for neutral 3*d* TMHs with nonrelativistic BMK are plotted in Fig. 2 for reference to the data in Table I.

According to BMK, the first two lowest multiplicities for ScH (Fig. A3[60]) are close in energy but differ in the bond length, so that the singlet is more stable at the shorter and the triplet at the longer bond length. On the contrary, TPSS overstabilizes the singlet at all distances. Only singlet multiplicity is reported in the previous works[1,18,47,79] including the WFT study by Koseki *et al.*[21] Two spin multiplicities are reported for VH at WFT (Ref. 20) (Fig. A4[60]). Both BMK and TPSS reproduce the ordering, although the spin gap in BMK is twice larger than that in WFT. The BMK result seems to be more reliable as it closely reproduces experimental D_e for the multiplicity of 5. The two multiplicities for MnH (Fig. A5[60]) are almost degenerate in both BMK and TPSS, while WFT favors $M=7$ by 11 kcal/mol. Unlike the other TMHs, MnH is found to have strong, more than 10%, spin contamination close to equilibrium bond length for $M=5$. The spin-contamination correction (detailed in the Appendix) stabilizes this spin state by 3.5 kcal/mol below $M=7$, in disagreement with WFT. The corrected BMK dissociation energy is, however, closer to the experimental value reported by Barone and Adamo.[47] Three multiplicities of CrH are reported at WFT (Ref. 19) (Fig. 1), all with different dissociation limits. Both WFT and DFT predict the ground state to have the multiplicity of 6. BMK and especially TPSS underestimate the spin gap at equilibrium, as compared to the *ab initio* results, while they reproduce it fairly well at the dissociation limit.

The energy difference between the high and low spin

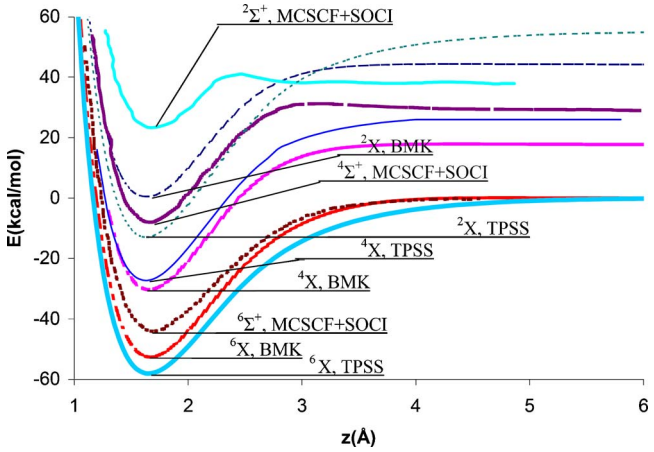

FIG. 1. (Color online) PECs of CrH with multiplicities of 2, 4, and 6 calculated by nonrelativistic TPSS, BMK, and WFT (Ref. 19) methods.

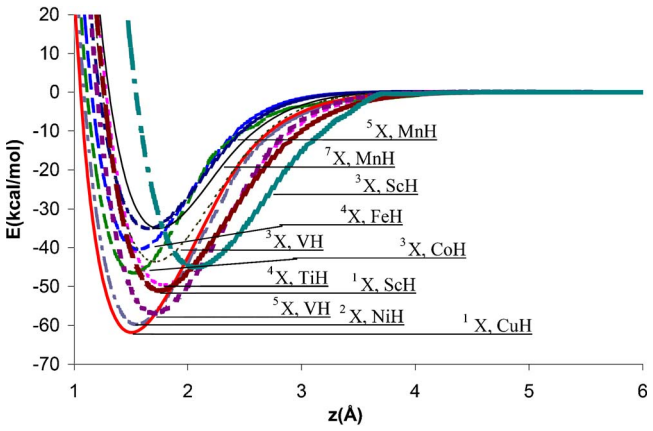

FIG. 2. (Color online) PECs of neutral TMH calculated by nonrelativistic BMK.

TABLE III. Dissociation energies (kcal/mol) of TMH cations and rms deviations from the experimental values.

	ScH+	TiH+	VH+	CrH+	MnH+	FeH+	CoH+	NiH+	CuH+	rms deviations	
Multiplicity	2	3	4	5	6	5	4	3	2	Set 1	Set 2
BS-TPSS	65.1	62.9	58.6	44.2	55.5	58.8	55.2	52.4	34.6	3.81	3.58
BS-BMK	57.8	55.7	48.4	37.0	45.3	54.5	50.2	35.0	22.6	1.43	1.14
SA-B3LYP[a]	57.5	62.0	48.5	36.0	49.3	58.0	53.9	43.2	27.2	2.03	1.89
MCPF[b]	54.40	51.0	47.0	27.8	40.8	49.1	40.7	36.4	15.9	1.22	1.29
Expt. set 1[a]	55.3	55.1	47.3	27.7	47.5	48.9	45.7	38.6	21.2		
Expt. set 2	56.3 ± 2[c]	54.3 ± 3[d]	48.3 ± 1[e]	31.6 ± 2[f]	47.5 ± 3[g]	48.9 ± 1[h]	45.7 ± 1[i]	38.7 ± 2[i]	21.2 ± 3[i]		

[a]Reference 47.
[b]Reference 79.
[c]Reference 85.
[d]Reference 92.
[e]Reference 86.
[f]Reference 87.
[g]Reference 88.
[h]References 89, 90, and 93.
[i]Reference 91.

states was studied previously by several authors and found to depend strongly on the fraction of HF exchange. This can be attributed to the fine balance between the negative HF exchange energy contribution from the electron of the same spin, which is opposite in sign to the electronic correlation contribution arising from the repulsion between any two electrons regardless of their spin. A method that includes the exchange and neglects the correlation (such as HF) will favor high multiplicities by maximizing the number of electrons with the same spin. To the contrary, self-interaction error in pure DFT favors low spin states. Attempts to improve the relative spin-state energy description of density functionals include hybrid DFT schemes as well as DFT+U.[80] It was recently shown that DFT+U is capable of providing the qualitatively correct splitting in low and high spin iron porphyrins[80] and FeO^+.[81] However, when the BS approach is adapted, the improvements obtained by the use of the Hubbard+U correction can be accomplished by improving the form of the DFT functional.[82] Conradie and Ghosh[83] studied Fe(+2) spin-crossover complexes and found that pure functionals such as BLYP, PW91, and BP86 unduly favor spin-coupled form (covalent description), while hybrid functionals such as B3LYP lean in the other direction. To correct the latter, they suggested reducing the amount of HF exchange in B3LYP from the standard 20% to 15%; the modified B3LYP functional has been found to give improved results. These calculations are in agreement with the recent review by Harvey.[84] He found an optimum exact exchange admixture of 15% to yield accurate results in many other cases. It appears that the large fraction of HF exchange is necessary for the correct prediction of the dissociation energies while a smaller fraction is in better agreement with experimentally observed spin gaps.

We observed spin contamination in almost all TM neutral and ionic hydrides at intermediate distances. Spin contamination at the equilibrium was found to be less than 10% for all hydrides except in the case of MnH.

B. Metal hydride cations

Dissociation energies for cationic hydrides in equilibrium geometry are reported in Table III. Comparisons with two sets of experimental data and some of the published WFT and DFT predictions are also given. The experimental dissociation energies from Refs. 85–93 are listed in Table III as set 2. Both set 2 and set 1 (compiled by Barone and Adamo[47]) were used to calculate the rms deviations for all theoretical values. Comparison with both the sets indicates that the BMK functional performs better than other XC functionals, while TPSS strongly overbinds in all cases. BMK values are superior to the best WFT data (when compared with new compilation), while hybrid B3LYP functionals demonstrate larger deviations. The deviations of predicted dissociation energies from experimental values (set 2) are plotted in Fig. A6.[60] One can see that WFT underestimates the bonding energies, TPSS overbinds, and BMK is bracketed by these values for all TMH cations except NiH^+. All deviations at the BMK level are within 6 kcal/mol.

TABLE IV. Equilibrium bond lengths (Å) of TMH cations and rms deviations from the experimental values.

	ScH+	TiH+	VH+	CrH+	MnH+	FeH+	CoH+	NiH+	CuH+	
Multiplicity	2	3	4	5	6	5	4	3	2	rms
BS-TPSS	1.775	1.695	1.632	1.600	1.598	1.568	1.540	1.487	1.512	0.018
BS-BMK	1.791	1.713	1.648	1.609	1.633	1.589	1.540	1.496	1.508	0.013
SA-B3LYP[a]	1.766	1.700	1.648	1.594	1.600	1.561	1.541	1.466	1.478	0.016
MCPF[b]	1.829	1.740	1.661	1.604	1.652	1.603	1.547	1.487	1.445	0.002
Expt.	1.83[c]		1.663[c]		1.645[c]	1.598[c]	1.54[c]		1.443[c]	

[a]Reference 47.
[b]Reference 79.
[c]Reference 75.

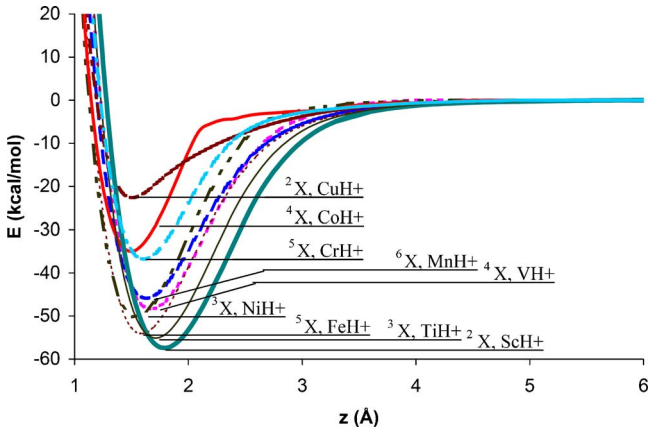

FIG. 3. (Color online) PECs of TMH cations calculated by nonrelativistic BMK.

Equilibrium bond lengths are reported in Table IV and Fig. A7.[60] Table IV includes experimental data[75] for six TMH systems out of nine in the 3*d* TM series. WFT performs considerably better than all the DFT methods for the bond length predictions, while BMK is superior to other functionals (except for the CuH^+ case).

PECs of MH cations for ScH^+, TiH^+, and CrH^+ in various multiplicities are reported in Figs. A8–A10[60] and compared with available MCSCF+SOCI curves.[27,28,94] All the curves for 3*d* TMH cations with nonrelativistic BMK are plotted in Fig. 3 for reference to the data in Table III.

C. Electronic structure and ionization potential (IP) of 3*d* transition metal hydrides

Table V reports the NBO analysis of BMK spin densities. The differences between the NBO analysis of BMK and TPSS are not significant, and we will only discuss BMK in the following. The naive description of TMs consists of 4*s* orbital involved in σ bonding and the remaining nonbonding *d* electrons coupled antiferromagnetically. Indeed, the highest spin state was found to be the most stable for all the neutral hydrides with two exceptions, ScH and MnH, where other multiplicities (1 and 7, respectively) are almost degenerate with the regular multiplicity (3 and 5) states. For that reason, we consider the high spin states first.

As one can see from Table V, this naive description is accurate only for NiH and CuH. For FeH, CoH, and CrH, *s* and *d* orbitals hybridize close to 50/50 to form the bond and for Sc, Ti, and V hydrides one of the unpaired electrons occupies the *s* orbital, and the covalent bond is formed by the *d* orbital of the majority (alpha) spin. The minority (beta) spin component of the covalent bond is still of *s* character in these molecules. One exception is MnH in the $M=7$ state, which in a simple picture, would have zero bond order with the bonding electrons uncoupled. From the NBO analysis of the majority spin electrons the bond is ionic, and minority spin is covalent (mostly formed by the *s* orbital). The low spin state of ScH has a lone pair on the *s* orbital. The remaining (VH, CrH, MnH) hydrides in the low spin states have nonbonding electron of the minority spin on the *s* orbital, while nonbonding electrons of majority spin are all on the *d* orbitals.

Dipole moments are reported in Table VI. BMK and TPSS values are compared with other WFT functionals for given multiplicities reported by Chong *et al.*[23] One can see from Table VI that BMK and TPSS values are not much different and are in close agreement with MCPF values for FeH, CoH, CuH, and MnH ($M=7$). BMK and TPSS slightly overestimate the dipole moment values for ScH, TiH, VH, and NiH in comparison to MCPF and are close to coupled pair functional (CPF) values (with the only exception of CrH).

Table VII reports the NBO analysis of BMK spin densities for MH cations. As can be seen from Table VII, the *s* electron is ionized during the formation of the cationic species in all cases. Also, for all TMH^+ systems, all nonbonding electrons are *d* electrons in both the spins (alpha and beta). In

TABLE V. TMH multiplicity (M), Alpha and Beta bonding and nonbonding orbital hybridization coefficients obtained from NBO analysis for the neutral TMHs calculated with BMK.

		Alpha (TM)										Beta (TM)								
			Bond (%)			Nonbonding (%)							Bond (%)			Nonbonding (%)				
Systems	M	Spin charge	*s*	*p*	*d*	1	2	3	4	5	6	Spin charge	*s*	*p*	*d*	1	2	3	4	5
ScH	1	0.26	18	5	77	*s*82						0.26	18	5	77	*s*82				
	3	−0.64	7	20	73	*d*100	*s*92					1.28	70	6	24					
TiH	4	−1.20	11	12	78	*d*100	*d*100	*s*89				1.76	70	5	25					
VH	3	−0.82	66	3	31	*d*100	*d*100	*d*100				1.32	10	11	80	*s*90				
	5	−1.79	19	5	76	*d*100	*d*100	*d*100	*s*81			2.25	72	3	25					
CrH	2	−0.37	82	2	16	*d*100	*d*100	*d*85				0.70	25	3	72	*d*100	*s*75			
	4	−1.34	59	2	39	*d*100	*d*100	*d*100	*d*100			1.79	13	7	80	*s*87				
	6	−2.39	44	2	54	*d*100	*d*100	*d*100	*d*100	*s*56	*d*44	2.78	71	3	26					
MnH	5	−1.92	91	2	7	*d*100	*d*100	*d*100	*d*100	*d*93		2.32	9	9	82	*s*91				
	7	−2.58	0	0	0	*d*100	*d*100	*d*100	*d*100	*d*77	*s*70	3.21	74	4	22					
FeH	4	−1.37	92	2	6	*d*100	*d*100	*d*100	*d*100	*d*94		1.67	41	2	57	*d*100	*s*59	*d*40		
CoH	3	−0.88	92	1	7	*d*100	*d*100	*d*100	*d*100	*d*93		1.13	55	1	44	*d*100	*d*100	*d*54	*s*45	
NiH	2	−0.36	93	1	5	*d*100	*d*100	*d*100	*d*100	*d*95		0.72	73	2	25	*d*100	*d*100	*d*100	*d*100	
CuH	1	0.15	92	2	6	*d*100	*d*100	*d*100	*d*100	*d*94		0.15	92	2	6	*d*100	*d*100	*d*100	*d*100	*d*94

TABLE VI. TMH Multiplicity (M), Dipole moments (Debye) for neutral TMHs calculated with BMK and TPSS compared with several WFT levels.

		Dipole Moments				
System	M	BMK	TPSS	SDCI[a]	CPF[a]	MCPF[a]
ScH	1	1.9	2.5	1.4	1.8	1.6
	3	2.6	2.8	2.0	2.6	2.4
TiH	4	2.6	2.6	1.9	2.3	2.2
VH	3	2.0	2.2			
	5	2.7	2.5	1.8	2.3	2.0
CrH	2	2.5	2.9			
	4	1.8	2.6			
	6	3.1	2.9	4.3	3.8	3.8
MnH	5	1.4	2.1			
	7	1.1	0.8	1.3	1.2	1.2
FeH	4	2.6	2.6	4.1	1.3	2.9
CoH	3	2.5	2.6	3.9	1.4	2.7
NiH	2	3.2	2.3	3.7	1.8	2.6
CuH	1	3.0	2.5	3.9	2.7	3.0

[a]Reference 23.

the majority spin, ScH^+, TiH^+, and VH^+ have s and d orbitals hybridizing close to 50/50, whereas in the remaining systems (MnH^+, FeH^+, CoH^+, NiH^+, and CuH^+) the s orbital was found to form covalent bond. In the case of CrH^+, the d orbital forms a covalent bond, which is due to its half-filled electronic configuration. The minority spin distributions for almost all the systems have close to 50/50 s and d hybridizations except for CuH^+, which shows covalent bond formation by the d orbital.

Table VIII gives the adiabatic and vertical IPs for BMK and TPSS along with experimental data. Our TPSS values of IP differ from the results recently reported by Riley and Merz,[44] with the same functional along with 11 other XC functionals. The differences (and larger deviations from experiment) obtained in their study are likely to originate from using the SA approach with default orbital guess. The average unsigned errors in our BS treatment are 0.141 and 0.269 eV for BMK and TPSS, respectively.

IV. CONCLUSION

We have used two XC functionals including explicit dependence on kinetic energy density (τ functionals) to study (both neutral and cationic) hydrides formed by 3d TMs (Sc–Cu). One of the functionals selected contained a large fraction of HF exchange (BMK), and another one was a pure DFT functional (TPSS). Watchers basis sets,[52] augmented with f functions by Hay,[53] were used. We have taken particular care in obtaining the SCF solution, including the stability analysis and Fermi smearing. In order to ensure the stability of the Slater determinant in the entire range of interatomic distances, the PECs were plotted and inspected for discontinuities. When found, the discontinuities were eliminated by using the orbitals of lower-energy SCF solution as initial guess to continue the curve smoothly. The spin orbitals at the dissociation limit were inspected and reordered if necessary.

A qualitatively correct description of the bond dissociation was ensured by allowing the spatial and spin symmetries to break. This resulted in appreciable spin contamination for some of the systems at equilibrium and all the systems at intermediate interatomic distances. In order to correct the spin-contamination effect on the energies, we developed a new approach. This approach differs from existing spin-correction schemes, which are based on the expectation value of the spin operator corresponding to the hypothetical

TABLE VII. Multiplicity (M) of TMH cations, Alpha and beta bonding and nonbonding orbital hybridization coefficients obtained from NBO analysis for the TMH cations calculated with BMK.

		Alpha (TM)										Beta (TM)								
			Bond (%)			Nonbonding (%)							Bond (%)			Nonbonding (%)				
Systems	M	Spin charge	s	p	d	1	2	3	4	5	6	Spin charge	s	p	d	1	2	3	4	5
ScH	2	0.22	33	1	66	d99						1.26	36	2	62					
TiH	3	−0.33	33	1	66	d100	d100					1.73	32	1	66					
VH	4	−0.89	30	1	69	d100	d100	d100				2.22	31	1	68					
CrH	5	−1.50	16	1	83	d100	d100	d100	d100			2.75	30	1	69					
MnH	6	−1.92	90	2	8	d100	d100	d100	d100	d92		3.14	29	1	70					
FeH	5	−1.34	93	2	5	d100	d100	d100	d100	d95		2.52	18	1	81	d100				
CoH	4	−0.88	95	2	3	d100	d100	d100	d100	d97		2.11	38	1	60	d100	d100			
NiH	3	−0.33	94	2	4	d100	d100	d100	d100	d96		1.42	17	1	83	d100	d100	d100		
CuH	2	0.26	94	3	3	d100	d100	d100	d100	d97		0.77	8	0	92	d100	d100	d100	d100	

TABLE VIII. Multiplicities for neutral TMH, their cations, adiabatic and vertical ionization potentials for TMH and their errors in comparison to experimental values.

				IP (eV)					Error		
			Expt.[a]	BMK		TPSS		SA-TPSS[b]			
System	*M* (TMH)	*M* (TMH^+)	Adiabatic	Adiabatic	Vertical	Adiabatic	Vertical	Adiabatic	BMK	TPSS	SA-TPSS[b]
ScH	1	2	6.209	6.090	6.371	6.165	6.169		−0.119	−0.044	
TiH	4	3	6.600	6.523	6.555	6.618	6.649	5.960	−0.077	0.018	−0.640
VH	5	4	6.363	6.116	6.330	6.224	6.266		−0.247	−0.139	
CrH	6	5	7.668	7.707	6.451	6.416	6.430		0.039	−1.252	
MnH	7	6	6.635	6.898	6.970	6.866	6.939	6.510	0.263	0.231	−0.125
FeH	4	5	7.374	7.467	7.479	7.677	7.905		0.093	0.303	
CoH	3	4	7.871	7.877	8.002	8.140	8.152	7.150	0.006	0.269	−0.721
NiH	2	3	8.531	8.195	8.206	8.635	8.653	7.490	−0.336	0.104	−1.041
CuH	1	2	9.447	9.359	9.361	9.387	9.408		−0.088	−0.060	

[a]From NIST database and Ref. 75.
[b]Reference 44.

noninteractive systems. Instead, our spin-correction scheme is based on the energy of high spin determinant built on the natural orbitals (NOs) of the total density, and its contribution is evaluated from the occupation numbers of these orbitals.

Based on the described protocol, we report BMK dissociation energies that are in better agreement with experiment than those obtained with high level WFT methods, published previously. This agreement with experiment deteriorates quickly when the fraction of the HF exchange in DFT functional is decreased. A higher fraction of HF exchange does not necessarily help, however, when the symmetry adapted (SA) unrestricted approach is employed. We found no improvements in dissociation energies when scalar relativistic effects are taken into account in the Douglas–Kroll approximation,[58] while bond distances showed twice lower rms deviations after relativistic corrections. We analyzed the electron spin densities using NBO population analysis and found that a simple description of the chemical bond in MHs as formed by the 4*s* orbital of the metal with 3*d* electrons keeping nonbonding character is rarely correct.

We also found that the average unsigned error for IPs is much lower (0.14 and 0.27 eV for BMK and TPSS, respectively) than that previously reported owing to the careful SCF protocol employed. However, the spin gaps for the systems with multiple spin states considered is in disagreement with the wave function data available even after the spin-contamination correction. This matter is presently under investigation and will be published elsewhere.

ACKNOWLEDGMENTS

This work is supported in part by the UCF start up grant. S.G. gratefully acknowledges the Interdisciplinary Information Sciences Laboratory (I2lab) fellowship. The computer time was generously provided by DOE NERSC, Stokes HPC facilities at UCF Institute for Simulation and Training (IST), and UCF I2lab. The authors are grateful to Annie Wu and Lee Chow for useful discussions and to an anonymous reviewer for the detailed list of suggested corrections.

APPENDIX: DERIVATION OF PAIRWISE SPIN-CONTAMINATION CORRECTION—A NEW APPROACH BASED ON CANONICAL NATURAL ORBITALS

Difficulties in DFT description of strongly correlated systems are based on the fact that DFT was derived based on the assumption of a nondegenerate system,[30,95] while multireference WFT methods are capable of taking degeneracy into account. DFT implementations use the KS formalism based on a single Slater determinant. Modifications to the formalism may thus be necessary to describe near degenerate cases. One of these modifications can be illustrated on the example of multiplet states of TM atoms. Ziegler *et al.*[96] suggested to calculate the energies of singlet and triplet states of TM atoms as linear combinations of energies for single Slater determinants built with different orbital occupations. They considered the four possible configurations of two electrons on two singly occupied MOs *a* and *b*, three triplets, and one singlet,

$$\|a_\alpha b_\alpha\|,\ \tfrac{1}{\sqrt{2}}(\|a_\alpha b_\beta\| + \|a_\beta b_\alpha\|),\ \|a_\beta b_\beta\|,\ \tfrac{1}{\sqrt{2}}(\|a_\alpha b_\beta\| - \|a_\beta b_\alpha\|). \tag{A1}$$

While electron density represented by determinant $D_1 = \|a_\alpha b_\alpha\|$ corresponds to the triplet energy

$$^{\mathrm{DFT}}E(D_1) = E_T(D_1), \tag{A2}$$

the energy of electron density represented by determinant $D_2 = \|a_\alpha b_\beta\|$ is the average of singlet and triplet energies:

$$^{\mathrm{DFT}}E(D_2) = \tfrac{1}{2}(E_T(D_2) + E_S(D_2)). \tag{A3}$$

The pure singlet energy can be then expressed as

$$E'_S = 2\,^{\mathrm{DFT}}E(D_1) - {}^{\mathrm{DFT}}E(D_2). \tag{A4}$$

This method was extended to higher atomic multiplets with partly occupied *p* shells[97,98] and *d* shells.[99–101] Although complex atomic orbitals and functionals dependent on current density are generally required to treat degenerate atomic multiplet states, Johnson *et al.*[101] recently suggested a set of rules to obtain accurate results with standard real orbitals and XC functionals.

Application of the sum rule Eq. (A3) to the molecular systems is complicated by the "symmetry dilemma."[102] While the SA spin-restricted orbitals form a proper basis for WFT treatment, a single Slater determinant built on these orbitals does not always correspond to the lowest-energy SCF solution. For instance, Benard[103] described several TM molecules where the SA solution incorrectly describes the electronic structure and lower-energy BS solutions exist. This issue had been extensively studied in the past,[103–106] and the general consensus seems to favor the lowest energy over the correct symmetry.

A clear advantage of the unrestricted (also known as spin-polarized or broken spin-symmetry) solution is the qualitatively correct description of the bond dissociation process.[102,107] Since the exact XC functional is not known, the UKS treatment improves approximate functionals by taking part of the static electron correlation into account. The situation can be seen as localization of α and β electrons on the left and right atoms of the dissociating bonds, respectively (left-right electron correlation). BS UKS thus describes the transition from a closed-shell system to a biradical smoothly, which is not possible with restricted open-shell KS.

Even for the simplest diatomic H_2 the restricted Kohn–Sham (RKS) approach does not describe bond dissociation correctly. It is possible, in principle, to obtain the correct dissociation limit if the exact XC functional was known. An attempt had been made to use linear response formalism to account for static electron correlation.[108] Although it helped in the dissociation limit, an unphysical dissociation barrier was obtained, presumably due to lack of double excitations in linear response. Another attempt used exact electron density obtained from WFT (full CI method) to restore the nearly exact XC potential.[109] That also resulted in unphysical barrier. It appears that the BS-UKS ansatz is the only approach in DFT applicable to systems with chemical bond dissociation. An attractive feature of the BS approach is that one obtains a "quasi-valence-bond–like" description with semilocalized magnetic orbitals that reflect the interacting singly occupied MOs of the subsystems. On the other hand, for a complicated many-electron molecule, it is difficult to extract the magnetic orbitals from the results of a spin-unrestricted calculation.[110]

A disadvantage of the UKS approach is that the spin-polarized Slater determinant is no longer an eigenfunction of the spin operator. Hence, the average value of $\langle \hat{S}^2 \rangle$ is not generally equal to the correct value of $S_z(S_z+1)$.[111] Here, S_z is $\frac{1}{2}$ of the difference in total numbers of α and β electrons. This situation is known as spin contamination and $\langle \hat{S}^2 \rangle$ is often used as its measure. The common rule[112] is to neglect spin contamination if $\langle \hat{S}^2 \rangle$ differs from $S_z(S_z+1)$ by less than 10%. As a result of spin contamination, molecular geometry may be distorted toward the high spin state one, spin density often becomes incorrect, and electron energy differs from the pure spin state ones. While some researchers argue that this spin contamination in DFT should be ignored,[102] others recognize it as a problem affecting the energy. Possible solutions to spin-contamination problem includes constrained DFT[46,113] and spin-contamination correction schemes.[114,115] The latter are discussed in detail below.

There are two general approaches to spin-contamination problem found in the literature: one is to project the UKS wave function of a noninteracting system onto eigenfunctions of the $\hat{S}^2$ operator, and another is to map the real system onto a model system described by a model Hamiltonian. An example of the projection approach is the (spin)-projected unrestricted Hartree-Fock (PUHF) method, implemented at the semiempirical level by Cory and Zerner.[116] While successful in the description of spin splitting in multicenter 3*d*-metal complexes, the PUHF method was found not to be size consistent, which resulted in errors of tens of kcal/mol for organic biradicals.[117–119] Orbital optimization after spin projection, such as in extended HF method[116] and in maximally paired Hartree–Fock method,[120] is expected to restore size consistency but faces substantial difficulties in practical implementation. Half-projected HF method offers a more practical solution at the expense of retaining higher order spin contamination.[121] Andrews *et al.*[122] proposed minimizing spin contamination, together with the total energy using the method of Langrange multipliers, and Yamanaka *et al.*[123] developed the new generalized Hartree–Fock–Slater method using noncollinear magnetic orbitals. An elegant formalism for optimization of spin-projected wave function, based on the strongly orthogonal geminal approach, was proposed recently,[124] but no DFT extension to it exists to date.

Another approach to treat the spin-contamination problem consists in mapping the model Hamiltonian onto results of *ab initio* calculations.[125] Typically, the Heizenberg–Dirac–Van Vleck phenomenological Hamiltonian is used (see Ref. 126 and references therein). This Hamiltonian describes the isotropic interaction between localized magnetic moments S_i and S_j as

$$\hat{H}_{\text{model}} = -\sum_{i,j} J_{ij} S_i S_j, \tag{A5}$$

where J_{ij} is the exchange coupling constant. For instance, in a system with two unpaired electrons, the coupling constant corresponds to singlet-triplet energy splitting:

$$J = E_S - E_T. \tag{A6}$$

A positive value of J corresponds to ferromagnetic, and a negative value corresponds to antiferromagnetic coupling. The mapping procedure consists in empirical adjustment of the coupling constant to match the multiplet energies obtained from WFT or experiment.[127–129] Since BS-DFT does not produce the energies of the pure spin states, the expression for J must account for spin contamination. The following three equations [Eqs. (A7)–(A9)] are the results obtained from these methods:

$$J = \frac{({}^{\text{DFT}}E_{\text{BS}} - {}^{\text{DFT}}E_T)}{S^2_{\text{max}}}, \tag{A7}$$

$$J = \frac{({}^{\text{DFT}}E_{\text{BS}} - {}^{\text{DFT}}E_T)}{S_{\text{max}}(S_{\text{max}}+1)}, \tag{A8}$$

$$J = \frac{({}^{\mathrm{DFT}}E_{\mathrm{BS}} - {}^{\mathrm{DFT}}E_T)}{\langle S^2\rangle_T - \langle S^2\rangle_{\mathrm{BS}}}. \tag{A9}$$

These three relations differ in their applicability, which depends on the degree of overlap between the two magnetic orbitals. Equation (A7) has been derived by Ginsberg,[130] Noodleman,[105] and Noodleman and Davidson[131] and is applied when the overlap of the magnetic orbitals is sufficiently small. Equation (A8) has been used by Bencini *et al.*[132] and Ruiz *et al.*[128] Illas and co-workers[126,127] justified the application of Eq. (A8) when the overlap is adequately large. Finally, Eq. (A9) has been developed by Yamaguchi and co-workers.[123,133] This can be reduced to Eqs. (A7) and (A8) in the weak and strong overlap regions, respectively.

Although Eqs. (A7)–(A9) only require the average value of spin operator and hence can be used with standard quantum-chemical programs with no code modifications, they did not lead to consistent agreement with experiment.[134] More complicated expressions for variable spin correction, including the dependence of J on overlap between corresponding spin-polarized orbitals p and q, were also derived recently.[110,135] This approach was shown to result in more accurate J values for Cu^{2+} binuclear complexes.[135,136] However, this variable spin-correction approach had not been applied to systems with two or more correlated electron pairs.

The expectation value of the spin operator $\langle\hat{S}^2\rangle$ obtained in standard quantum-chemical programs corresponds to the hypothetical system of noninteractive electrons, introduced in the KS approach, rather than the physical system of interest. The correct $\langle\hat{S}^2\rangle$ can be expressed, however, though the two-particle density matrix.[137,138] The $\langle\hat{S}^2\rangle$ values in the cases studied were found to be up to one order of magnitude greater than in the noninteracting case depending on the system. Alternatively, $\langle\hat{S}^2\rangle$ can be calculated in terms of the overlap of the spatial parts of the corresponding orbitals.[139]

Here we propose an alternative approach to variable spin correction based on canonical natural orbitals (NOs).[119] First, let us consider a diatomic system AB with one correlated electron pair, such as stretched H_2 molecule. We assume that the RKS formalism yields a higher energy for this system than for the unrestricted one, as in the case of the H_2 molecule far from equilibrium. The UKS description produces the NOs a and b as eigenvectors of the total density matrix with the orbital occupation numbers n_a and n_b as the corresponding eigenvalues. We further assume that $n_a < n_b$, which means that orbital a is antibonding and orbital b is bonding NO. They are SA, i.e., a is Σ_u and b is Σ_g in the case of the H_2 molecule. The corresponding spin-polarized BS orbitals p and q can be expressed[140] as a linear combination of a and b using polarization parameter λ:

$$p = \frac{1}{\sqrt{1+\lambda^2}}(b + \lambda a), \quad q = \frac{1}{\sqrt{1+\lambda^2}}(b - \lambda a). \tag{A10}$$

This parameter is determined by the occupation numbers n_a and n_b as shown below. If alpha and beta electrons are localized on different parts of the molecule and do not overlap, the polarization parameter become unity and we arrive to Noodleman's weak interaction limit. In the general case of a many-electron system, the orbitals of the alpha set, besides being orthogonal to each other, are also orthogonal to the orbitals of the beta set for a single exception of the corresponding beta orbital. The spin-polarized orbitals obtained with the most standard quantum chemistry codes do not possess this property, which is why one has to produce the corresponding spin-polarized orbitals from NOs. The BS solution can still be written as the Slater determinant in the basis of these corresponding orbitals as

$$\mathrm{BS} = 1/\sqrt{2}\|p_\alpha q_\beta\| = \frac{1}{\sqrt{2}}\begin{Vmatrix} p_1\alpha_1 p_2\alpha_2 \\ q_1\beta_1 q_2\beta_2 \end{Vmatrix}, \tag{A11}$$

where indices 1 and 2 mark coordinates of the electrons. Substitution of the corresponding orbitals from Eq. (A10) into Eq. (A11) separates the pure singlet and triplet components:

$$\mathrm{BS} = \frac{1}{\sqrt{2}}\begin{Vmatrix} p_1\alpha_1 p_2\alpha_2 \\ q_1\beta_1 q_2\beta_2 \end{Vmatrix} = \frac{1}{(1+\lambda^2)}S + \frac{\lambda}{(1+\lambda^2)}T \tag{A12}$$

$$= \frac{1}{(1+\lambda^2)}(b_1b_2 - \lambda^2 a_1a_2)\frac{\alpha_1\beta_2 - \beta_1\alpha_2}{\sqrt{2}} + \frac{\lambda}{(1+\lambda^2)}(a_1b_2 - b_1a_2)\frac{\alpha_1\beta_2 + \beta_1\alpha_2}{\sqrt{2}}, \tag{A13}$$

The first term in this expression contains the linear combination of the two closed-shell singlets, the lower closed-shell singlet S_1:

$$S_1 = b_1b_2\frac{\alpha_1\beta_2 - \beta_1\alpha_2}{\sqrt{2}}, \tag{A14}$$

and the higher closed-shell singlet S_2:

$$S_2 = a_1a_2\frac{\alpha_1\beta_2 - \beta_1\alpha_2}{\sqrt{2}}, \tag{A15}$$

while the second term is proportional to one of the possible triplet states: $T = T_0\sqrt{2}$,

$$T_0 = \frac{(a_1b_2 - b_1a_2)}{\sqrt{2}}\frac{(\alpha_1\beta_2 + \beta_1\alpha_2)}{\sqrt{2}}. \tag{A16}$$

This triplet contribution is the reason why the UKS solution is spin contaminated. Therefore, we are looking to extract the energy of the singlet term from the BS energy E_{BS} using the energy of the triplet. The expectation value of the KS operator $\hat{H}$ then becomes

$$E_{\mathrm{BS}} = \langle\mathrm{BS}|\hat{H}|\mathrm{BS}\rangle = \frac{1}{(1+\lambda^2)^2}\langle S|\hat{H}|S\rangle + \frac{\lambda^2}{(1+\lambda^2)^2}\langle T|\hat{H}|T\rangle + \frac{\lambda}{(1+\lambda^2)^2}(\langle S|\hat{H}|T\rangle + \langle T|\hat{H}|S\rangle). \tag{A17}$$

The last two terms in Eq. (A17) vanish due to the orthogonality of the S and T states, introduced in Eq. (A12). Using

normalization condition and substituting Eq. (A18) into Eq. (A12), one can obtain

$$\langle S|S\rangle = \langle b_1 b_2 - \lambda^2 a_1 a_2 | b_1 b_2 - \lambda^2 a_1 a_2\rangle = 1 + \lambda^4, \tag{A18}$$

$$\mathrm{BS} = \frac{\sqrt{1+\lambda^4}}{1+\lambda^2} S_0 + \frac{\lambda\sqrt{2}}{1+\lambda^2} T_0, \tag{A19}$$

where

$$S_0 = \frac{S}{\sqrt{1+\lambda^4}} = \frac{1}{\sqrt{1+\lambda^4}}(S_1 + \lambda^2 S_2). \tag{A20}$$

Hence, the BS UKS energy can be written in terms of renormalized singlet and triplet S_0 and T_0 as

$$E_{\mathrm{BS}} = \frac{1+\lambda^4}{(1+\lambda^2)^2}\langle S_0|\hat{H}|S_0\rangle + \frac{2\lambda^2}{(1+\lambda^2)^2}\langle T_0|\hat{H}|T_0\rangle, \tag{A21}$$

In the nonrelativistic case, the energy of the triplet T_0 is the same as the energy E_T for the single determinant triplet T_1,

$$E_T = \langle T_1|\hat{H}|T_1\rangle = \langle T_0|\hat{H}|T_0\rangle. \tag{A22}$$

Then the energy E_S of the pure singlet S_0 can be found from Eq. (A22) as

$$E_{S_0} = \frac{(1+\lambda^2)^2}{1+\lambda^4} E_{\mathrm{BS}} - \frac{2\lambda^2}{1+\lambda^4} E_T. \tag{A23}$$

This energy includes the nondynamic electron correlation effects arising from the mixing of the S_1 and S_2 states. In order to relate the polarization parameter λ to the occupation numbers n_a and n_b, we can expand the electron density matrix in the basis of the a and b orbitals,

$$\rho(\mathrm{BS}) = \begin{bmatrix} n_a & 0 \\ 0 & n_b \end{bmatrix}, \quad \rho(S_1) = \begin{bmatrix} 0 & 0 \\ 0 & 2 \end{bmatrix},$$
$$\rho(S_2) = \begin{bmatrix} 2 & 0 \\ 0 & 0 \end{bmatrix}, \quad \rho(T_0) = \begin{bmatrix} 1 & 0 \\ 0 & 1 \end{bmatrix}. \tag{A24}$$

From Eqs. (A19) and (A20)

$$\rho(\mathrm{BS}) = \frac{1}{1+\lambda^2}\rho(S_1) + \frac{\lambda^4}{(1+\lambda^2)^2}\rho(S_2) + \frac{2\lambda^2}{(1+\lambda^2)^2}\rho(T_0). \tag{A25}$$

Then

$$n_a = \frac{2\lambda^4}{(1+\lambda^2)^2} + \frac{2\lambda^2}{(1+\lambda^2)^2} = \frac{2\lambda^2}{1+\lambda^2}, \tag{A26}$$

$$n_b = \frac{2}{(1+\lambda^2)^2} + \frac{2\lambda^2}{(1+\lambda^2)^2} = \frac{2}{1+\lambda^2}. \tag{A27}$$

Finally,

$$\lambda = \sqrt{2/n_b - 1}, \tag{A28}$$

$$E_{S_0} = \frac{4}{2n_b^2 + 4n_b + 4} E_{\mathrm{BS}} - \frac{4n_b - 2n_b^2}{2n_b^2 + 4n_b + 4} E_T. \tag{A29}$$

Thus, for a system with one correlated electron pair one can obtain the pure singlet energy expressed in terms of the energy of the BS UKS solution, the occupation number of the bonding NO, and the energy of the triplet built on these bonding and antibonding NOs (as opposed to the self-consistent KS orbitals). This expression is applicable to two-electron systems as well as to the systems, which have in addition the unpolarized electron core or ferromagnetically coupled unpaired electrons.

We will turn next to the systems with two correlated electron pairs, In that case, Eq. (A17) can be written as

$$E_{\mathrm{BS}} = \langle \mathrm{BS}_1\mathrm{BS}_2|\hat{H}_2|\mathrm{BS}_1\mathrm{BS}_2\rangle. \tag{A30}$$

Using Eq. (A19),

$$\mathrm{BS}_1\mathrm{BS}_2 = \left(\frac{\sqrt{1+\lambda_1^4}}{(1+\lambda_1^2)} S_{01} + \frac{\sqrt{2}\lambda_1}{(1+\lambda_1^2)} T_{01}\right) \times \left(\frac{\sqrt{1+\lambda_2^4}}{(1+\lambda_2^2)} S_{02} + \frac{\sqrt{2}\lambda_2}{(1+\lambda_2^2)} T_{02}\right) \tag{A31}$$

$$= \frac{1}{(1+\lambda_1^2)(1+\lambda_2^2)}(\sqrt{1+\lambda_1^4}\sqrt{1+\lambda_2^4} S_{01}S_{02} + \sqrt{2}\lambda_2\sqrt{1+\lambda_1^4} T_{02}S_{01} + \sqrt{2}\lambda_1\sqrt{1+\lambda_2^4} T_{01}S_{02} + 2\lambda_1\lambda_2 T_{01}T_{02}). \tag{A32}$$

Simplifying the above equation by replacing S_{01} and S_{02}:

$$S_{01} = \left(\mathrm{BS}_1 - \frac{\sqrt{2}\lambda_1}{(1+\lambda_1^2)} T_{01}\right)\frac{(1+\lambda_1^2)}{\sqrt{1+\lambda_1^4}}, \tag{A33}$$

$$S_{02} = \left(\mathrm{BS}_2 - \frac{\sqrt{2}\lambda_2}{(1+\lambda_2^2)} T_{02}\right)\frac{(1+\lambda_2^2)}{\sqrt{1+\lambda_2^4}} \tag{A34}$$

$$= \frac{1}{(1+\lambda_1^2)(1+\lambda_2^2)}(\sqrt{1+\lambda_1^4}\sqrt{1+\lambda_2^4} S_{01}S_{02} + \sqrt{2}\lambda_2(1+\lambda_1^2) T_{02}\mathrm{BS}_1 + \sqrt{2}\lambda_1(1+\lambda_2^2) T_{01}\mathrm{BS}_2 + 2\lambda_1\lambda_2 T_{01}T_{02}). \tag{A35}$$

Hence, the BS UKS energy can be written in terms of renormalized singlet, triplet, and mixtures of the triplet and the BS state, $S_{01}S_{02}$, $T_{01}T_{02}$, $T_{02}\mathrm{BS}_1$, and $T_{01}\mathrm{BS}_2$, as

$$E_{\mathrm{BS}} = \frac{(1+\lambda_1^4)(1+\lambda_2^4)}{(1+\lambda_1^2)^2(1+\lambda_2^2)}\langle S_{01}S_{02}|\hat{H}|S_{01}S_{02}\rangle + \frac{2\lambda_2^2(1+\lambda_1^2)^2}{(1+\lambda_1^2)^2(1+\lambda_2^2)}\langle T_{02}\mathrm{BS}_1|\hat{H}|T_{02}\mathrm{BS}_1\rangle + \frac{2\lambda_1^2(1+\lambda_2^2)^2}{(1+\lambda_1^2)^2(1+\lambda_2^2)}\langle T_{01}\mathrm{BS}_2|\hat{H}|T_{01}\mathrm{BS}_2\rangle - \frac{4\lambda_1^2\lambda_2^2}{(1+\lambda_1^2)^2(1+\lambda_2^2)}\langle T_{01}T_{02}|\hat{H}|T_{01}T_{02}\rangle. \tag{A36}$$

This expression includes one unknown energy value E_{S_0}, one converged SCF energy for broken symmetry system, and three energies for high spin systems

$$E_{\mathrm{BS}}(1+\lambda_1^2)^2(1+\lambda_2^2)^2 = (1+\lambda_1^4)(1+\lambda_2^4)E_{S_0} + 2\lambda_2^2(1+\lambda_1^2)^2E_{T_{02}\mathrm{BS}_1} + 2\lambda_1^2(1+\lambda_2^2)^2E_{T_{01}\mathrm{BS}_2} - 4\lambda_1^2\lambda_2^2E_{T_{01}T_{02}}. \quad \text{(A37)}$$

Then the energy E_{S_0} of the pure singlet $S_{01}S_{02}$ can be found from Eq. (A37) as

$$E_{S_0} = \frac{1}{(1+\lambda_1^4)(1+\lambda_2^4)}(E_{\mathrm{BS}}(1+\lambda_1^2)^2(1+\lambda_2^2)^2 - 2\lambda_2^2(1+\lambda_1^2)^2E_{T_{02}\mathrm{BS}_1} - 2\lambda_1^2(1+\lambda_2^2)^2E_{T_{01}\mathrm{BS}_2} + 4\lambda_1^2\lambda_2^2E_{T_{01}T_{02}}). \quad \text{(A38)}$$

Here, we derive an expression to extract the energy of the pure singlet state from the energy of the BS DFT description of the low spin state and energies of the high spin states: pentuplet and two spin-contaminated triplets. Thus, unlike spin-contamination correction schemes by Noodleman[105] and Yamaguchi *et al.*,[133] spin correction is introduced for each correlated electron pair individually and therefore is expected to give more accurate results.

[1] F. Furche and J. P. Perdew, J. Chem. Phys. **124**, 044103 (2006).
[2] J. G. Harrison, J. Chem. Phys. **79**, 2265 (1983).
[3] K. P. Jensen, B. O. Roos, and U. Ryde, J. Chem. Phys. **126**, 014103 (2007).
[4] J. A. M. Simoes and J. L. Beauchamp, Chem. Rev. (Washington, D.C.) **90**, 629 (1990).
[5] J. H. Walker, T. E. H. Walker, and H. P. Kelly, J. Chem. Phys. **57**, 2094 (1972).
[6] K. Tanaka, M. Sekiya, and M. Yoshimine, J. Chem. Phys. **115**, 4558 (2001).
[7] M. Sodupe, J. M. Lluch, A. Oliva, F. Illas, and J. Rubio, J. Chem. Phys. **92**, 2478 (1990).
[8] P. S. Bagus and C. Bjorkman, Phys. Rev. A **23**, 461 (1981).
[9] M. R. A. Blomberg, P. E. M. Siegbahn, and B. O. Roos, Mol. Phys. **47**, 127 (1982).
[10] C. M. Marian, M. R. A. Blomberg, and P. E. M. Siegbahn, J. Chem. Phys. **91**, 3589 (1989).
[11] R. Pouamerigo, M. Merchan, I. Nebotgil, P. A. Malmqvist, and B. O. Roos, J. Chem. Phys. **101**, 4893 (1994).
[12] J. Anglada, P. J. Bruna, and S. D. Peyerimhoff, Mol. Phys. **69**, 281 (1990).
[13] C. W. Bauschlicher, J. Phys. Chem. **92**, 3020 (1988).
[14] D. G. Dai and K. Balasubramanian, J. Mol. Spectrosc. **161**, 455 (1993).
[15] M. Freindorf, C. M. Marian, and B. A. Hess, J. Chem. Phys. **99**, 1215 (1993).
[16] K. Raghavachari, K. K. Sunil, and K. D. Jordan, J. Chem. Phys. **83**, 4633 (1985).
[17] S. P. Walch and C. W. Bauschlicher, J. Chem. Phys. **78**, 4597 (1983).
[18] A. B. Kunz, M. P. Guse, and R. J. Blint, J. Phys. B **8**, L358 (1975).
[19] S. Koseki, T. Matsushita, and M. S. Gordon, J. Phys. Chem. A **110**, 2560 (2006).
[20] S. Koseki, Y. Ishihara, D. G. Fedorov, H. Umeda, M. W. Schmidt, and M. S. Gordon, J. Phys. Chem. A **108**, 4707 (2004).
[21] S. Koseki, Y. Ishihara, H. Umeda, D. G. Fedorov, and M. S. Gordon, J. Phys. Chem. A **106**, 785 (2002).
[22] B. Meunier, Chem. Rev. (Washington, D.C.) **92**, 1411 (1992).
[23] D. P. Chong, S. R. Langhoff, C. W. Bauschlicher, and S. P. Walch, J. Chem. Phys. **85**, 2850 (1986).
[24] G. Ohanessian and W. A. Goddard, Acc. Chem. Res. **23**, 386 (1990).
[25] M. Sodupe, J. M. Lluch, A. Oliva, F. Illas, and J. Rubio, J. Chem. Phys. **90**, 6436 (1989).
[26] J. Anglada, P. J. Bruna, and F. Grein, J. Chem. Phys. **92**, 6732 (1990).
[27] A. E. Alvaradoswaisgood, J. Allison, and J. F. Harrison, J. Phys. Chem. **89**, 2517 (1985).
[28] A. Mavridis and J. R. Harrison, J. Chem. Soc., Faraday Trans. 2 **85**, 1391 (1989).
[29] W. Kohn, A. D. Becke, and R. G. Parr, J. Phys. Chem. **100**, 12974 (1996).
[30] W. Kohn and L. J. Sham, Phys. Rev. **140**, A1133 (1965).
[31] P. Geerlings, F. De Proft, and W. Langenaeker, Chem. Rev. (Washington, D.C.) **103**, 1793 (2003).
[32] T. Bredow, G. Geudtner, and K. Jug, J. Comput. Chem. **22**, 861 (2001).
[33] D. Porezag, T. Frauenheim, T. Kohler, G. Seifert, and R. Kaschner, Phys. Rev. B **51**, 12947 (1995).
[34] L. G. M. Pettersson, C. W. Bauschlicher, S. R. Langhoff, and H. Partridge, J. Chem. Phys. **87**, 481 (1987).
[35] A. D. Becke, Phys. Rev. A **38**, 3098 (1988).
[36] A. D. Becke, J. Chem. Phys. **104**, 1040 (1996).
[37] S. Hirata, H. Torii, and M. Tasumi, Phys. Rev. B **57**, 11994 (1998).
[38] K. N. Kudin, G. E. Scuseria, and R. L. Martin, Phys. Rev. Lett. **89**, 266402 (2002).
[39] A. D. Becke, J. Chem. Phys. **98**, 5648 (1993).
[40] C. Adamo and V. Barone, J. Chem. Phys. **110**, 6158 (1999).
[41] T. Ziegler and J. Li, Can. J. Chem. **72**, 783 (1994).
[42] V. Barone, C. Adamo, and F. Mele, Chem. Phys. Lett. **249**, 290 (1996).
[43] J. Baker and P. Pulay, J. Comput. Chem. **24**, 1184 (2003).
[44] K. E. Riley and K. M. Merz, J. Phys. Chem. A **111**, 6044 (2007).
[45] N. E. Schultz, Y. Zhao, and D. G. Truhlar, J. Phys. Chem. A **109**, 11127 (2005).
[46] C. V. Diaconu, A. E. Cho, J. D. Doll, and D. L. Freeman, J. Chem. Phys. **121**, 10026 (2004).
[47] V. Barone and C. Adamo, Int. J. Quantum Chem. **61**, 443 (1997).
[48] J. M. Tao, J. P. Perdew, V. N. Staroverov, and G. E. Scuseria, Phys. Rev. Lett. **91**, 146401 (2003).
[49] A. D. Boese and J. M. L. Martin, J. Chem. Phys. **121**, 3405 (2004).
[50] M. M. Quintal, A. Karton, M. A. Iron, A. D. Boese, and J. M. L. Martin, J. Phys. Chem. A **110**, 709 (2006).
[51] M. J. Frisch, G. W. Trucks, H. B. Schlegel *et al.*, GAUSSIAN03, Revision D.01 (Gaussian, Wallingford, CT, 2004).
[52] A. J. Wachters, J. Chem. Phys. **52**, 1033 (1970).
[53] P. J. Hay, J. Chem. Phys. **66**, 4377 (1977).
[54] J. Harris, Phys. Rev. B **31**, 1770 (1985).
[55] A. D. Rabuck and G. E. Scuseria, J. Chem. Phys. **110**, 695 (1999).
[56] G. Schaftenaar and J. H. Noordik, J. Comput.-Aided Mol. Des. **14**, 123 (2000).
[57] A. E. Reed and F. Weinhold, Isr. J. Chem. **31**, 277 (1991).
[58] M. Douglas and N. M. Kroll, Ann. Phys. **82**, 89 (1974).
[59] G. Jansen and B. A. Hess, Phys. Rev. A **39**, 6016 (1989).
[60] See EPAPS Document No. E-JCPSA6-129-026839 for detailed information on binding energies and bond lengths for neutral TMH and their cations and PECs of various TMH and their cations in various spin states, calculated by DFT methods and compared with WFT results. For more information on EPAPS, see http://www.aip.org/pubservs/epaps.html.
[61] A. Kant and K. A. Moon, High. Temp. Sci. **11**, 52 (1979); E. R. Fisher and P. B. Armentrout, J. Phys. Chem. **94**, 1674 (1990).
[62] Y. M. Chen, D. E. Clemmer, and P. B. Armentrout, J. Chem. Phys. **95**, 1228 (1991).
[63] A. Kant and K. A. Moon, High. Temp. Sci. **14**, 23 (1981).
[64] Y. M. Chen, D. E. Clemmer, and P. B. Armentrout, J. Chem. Phys. **98**, 4929 (1993).
[65] L. S. Sunderlin and P. B. Armentrout, J. Phys. Chem. **94**, 3589 (1990).
[66] R. H. Schultz and P. B. Armentrout, J. Chem. Phys. **94**, 2262 (1991).
[67] R. L. Martin and P. J. Hay, J. Chem. Phys. **75**, 4539 (1981).
[68] H. T. Jeng and C. S. Hsue, Phys. Rev. B **62**, 9876 (2000).
[69] W. L. Zou and W. J. Liu, J. Comput. Chem. **28**, 2286 (2007).
[70] S. A. Kadavathu, S. Lofgren, and R. Scullman, Phys. Scr. **35**, 277 (1987).
[71] I. E. Gordon, R. J. Le Roy, and P. F. Bernath, J. Mol. Spectrosc. **237**, 11 (2006).
[72] C. W. Bauschlicher and S. R. Langhoff, Chem. Phys. Lett. **145**, 205 (1988).
[73] C. E. Moore, *Atomic Energy Levels*, Natl. Bur. Stand. (U.S.) Circ. No. 35, Vol. I–III (1971). (U.S. GPO, Washington, D.C., 1949).
[74] G. Herzberg, *Spectra of Diatomic Molecules*, 2nd ed. (D. Van Nostrand Company, Inc., Princeton, NJ, 1950).
[75] A. Dedieu, *Transition Metal Hydrides* (VCH, France, 1990).

[76] J. A. Gray, M. G. Li, T. Nelis, and R. W. Field, J. Chem. Phys. **95**, 7164 (1991).
[77] S. P. Beaton, K. M. Evenson, and J. M. Brown, J. Mol. Spectrosc. **164**, 395 (1994).
[78] R. S. Ram, P. F. Bernath, and J. W. Brault, J. Mol. Spectrosc. **113**, 269 (1985).
[79] J. F. Harrison, Chem. Rev. (Washington, D.C.) **100**, 679 (2000).
[80] D. A. Scherlis, M. Cococcioni, P. Sit, and N. Marzari, J. Phys. Chem. B **111**, 7384 (2007).
[81] H. J. Kulik, M. Cococcioni, D. A. Scherlis, and N. Marzari, Phys. Rev. Lett. **97**, 103001 (2006).
[82] A. Sorkin, M. A. Iron, and D. G. Truhlar, J. Chem. Theory Comput. **4**, 307 (2008).
[83] J. Conradie and A. Ghosh, J. Phys. Chem. B **111**, 12621 (2007).
[84] J. N. Harvey, *Principles and Applications of Density Functional Theory in Inorganic Chemistry I* (Springer, Germany, 2004), Vol. 112, p. 151.
[85] J. L. Elkind, L. S. Sunderlin, and P. B. Armentrout, J. Phys. Chem. **93**, 3151 (1989).
[86] J. L. Elkind and P. B. Armentrout, J. Phys. Chem. **89**, 5626 (1985).
[87] J. L. Elkind and P. B. Armentrout, J. Chem. Phys. **86**, 1868 (1987).
[88] J. L. Elkind and P. B. Armentrout, J. Chem. Phys. **84**, 4862 (1986).
[89] J. L. Elkind and P. B. Armentrout, J. Phys. Chem. **90**, 5736 (1986).
[90] L. F. Halle, F. S. Klein, and J. L. Beauchamp, J. Am. Chem. Soc. **106**, 2543 (1984).
[91] J. L. Elkind and P. B. Armentrout, J. Phys. Chem. **90**, 6576 (1986).
[92] J. L. Elkind and P. B. Armentrout, Int. J. Mass Spectrom. Ion Process. **83**, 259 (1988).
[93] J. L. Elkind and P. B. Armentrout, J. Am. Chem. Soc. **108**, 2765 (1986).
[94] A. E. Alvaradoswaisgood and J. F. Harrison, J. Phys. Chem. **89**, 5198 (1985).
[95] P. Hohenberg and W. Kohn, Phys. Rev. **136**, B864 (1964).
[96] T. Ziegler, A. Rauk, and E. J. Baerends, Theor. Chim. Acta **43**, 261 (1977).
[97] U. Vonbarth, Phys. Rev. A **20**, 1693 (1979).
[98] M. Lannoo, G. A. Baraff, and M. Schluter, Phys. Rev. B **24**, 943 (1981).
[99] J. H. Wood, J. Phys. B **13**, 1 (1980).
[100] M. Weinert, R. E. Watson, and G. W. Fernando, Phys. Rev. A **66**, 032508 (2002).
[101] E. R. Johnson, R. M. Dickson, and A. D. Becke, J. Chem. Phys. **126**, 184104 (2007).
[102] J. P. Perdew, A. Savin, and K. Burke, Phys. Rev. A **51**, 4531 (1995).
[103] M. Benard, J. Chem. Phys. **71**, 2546 (1979).
[104] P. J. Hay, J. C. Thibeault, and R. Hoffmann, J. Am. Chem. Soc. **97**, 4884 (1975).
[105] L. Noodleman, J. Chem. Phys. **74**, 5737 (1981).
[106] A. P. Gingsberg, Inorg. Chim. Acta, Rev. **5**, 45 (1971).
[107] C. D. Sherrill, M. S. Lee, and M. Head-Gordon, Chem. Phys. Lett. **302**, 425 (1999).
[108] M. Fuchs, Y. M. Niquet, X. Gonze, and K. Burke, J. Chem. Phys. **122**, 094116 (2005).
[109] M. J. G. Peach, A. M. Teale, and D. J. Tozer, J. Chem. Phys. **126**, 244104 (2007).
[110] F. Neese, J. Phys. Chem. Solids **65**, 781 (2004).
[111] E. R. Davidson and A. E. Clark, Phys. Chem. Chem. Phys. **9**, 1881 (2007).
[112] D. Young, *Computational Chemistry: A Practical Guide for Applying Techniques to Real World Problems* (Wiley, New York, 2001).
[113] Q. Wu and T. Van Voorhis, Phys. Rev. A **72**, 024502 (2005).
[114] T. Lovell, W. G. Han, T. Q. Liu, and L. Noodleman, J. Am. Chem. Soc. **124**, 5890 (2002).
[115] R. Takeda, S. Yamanaka, and K. Yamaguchi, Int. J. Quantum Chem. **106**, 3303 (2006).
[116] M. G. Cory and M. Zerner, J. Phys. Chem. A **103**, 7287 (1999).
[117] E. R. Davidson and A. E. Clark, Int. J. Quantum Chem. **103**, 1 (2005).
[118] A. I. Krylov, J. Chem. Phys. **113**, 6052 (2000).
[119] P. M. Kozlowski and P. Pulay, Theor. Chem. Acc. **100**, 12 (1998).
[120] U. Kaldor, Phys. Rev. A **1**, 1586 (1970).
[121] Y. G. Smeyers, *Advances in Quantum Chemistry* (Academic, USA, 2000), Vol. 36, p. 253.
[122] J. S. Andrews, D. Jayatilaka, R. G. A. Bone, N. C. Handy, and R. D. Amos, Chem. Phys. Lett. **183**, 423 (1991).
[123] S. Yamanaka, D. Yamaki, Y. Shigeta, H. Nagao, Y. Yoshioka, N. Suzuki, and K. Yamaguchi, Int. J. Quantum Chem. **80**, 664 (2000).
[124] V. A. Rassolov and F. Xu, J. Chem. Phys. **126**, 234112 (2007).
[125] I. Ciofini, C. Adamo, V. Barone, G. Berthier, and A. Rassat, Chem. Phys. **309**, 133 (2005).
[126] I. P. R. Moreira and F. Illas, Phys. Chem. Chem. Phys. **8**, 1645 (2006).
[127] F. Illas and R. L. Martin, J. Chem. Phys. **108**, 2519 (1998).
[128] E. Ruiz, J. Cano, S. Alvarez, and P. Alemany, J. Comput. Chem. **20**, 1391 (1999).
[129] F. Neese, J. Am. Chem. Soc. **128**, 10213 (2006).
[130] A. P. Ginsberg, J. Am. Chem. Soc. **102**, 111 (1980).
[131] L. Noodleman and E. R. Davidson, Chem. Phys. **109**, 131 (1986).
[132] A. Bencini, D. Gatteschi, F. Totti, D. N. Sanz, J. A. Mc Cleverty, and M. D. Ward, J. Phys. Chem. A **102**, 10545 (1998).
[133] K. Yamaguchi, Y. Takahara, T. Fueno, and K. N. Houk, Theor. Chim. Acta **73**, 337 (1988).
[134] E. Rudberg, P. Salek, Z. Rinkevicius, and H. Agren, J. Chem. Theory Comput. **2**, 981 (2006).
[135] M. E. Ali and S. N. Datta, J. Phys. Chem. A **110**, 2776 (2006).
[136] M. E. Ali and S. N. Datta, J. Mol. Struct.: THEOCHEM **775**, 19 (2006).
[137] J. H. Wang, A. D. Becke, and V. H. Smith, J. Chem. Phys. **102**, 3477 (1995).
[138] A. J. Cohen, D. J. Tozer, and N. C. Handy, J. Chem. Phys. **126**, 214104 (2007).
[139] I. Theophilou, S. Thanos, and A. K. Theophilou, J. Chem. Phys. **127**, 234103 (2007).
[140] D. M. Chipman, Theor. Chim. Acta **82**, 93 (1992).